Title

Aging of human short-wave cone pathways

Journal

Proceedings of the National Academy of Sciences of the United States of America, 109(33)

ISSN

0027-8424

Authors

Shinomori, Keizo
Werner, John S

Publication Date

2012-08-14

DOI

10.1073/pnas.1119770109

Peer reviewed

Aging of human short-wave cone pathways

Keizo Shinomori[a] and John S. Werner[b,1]

[a]School of Information, Kochi University of Technology, 185 Tosayamada-Miyanokuchi, Kami, Kochi 782-8502, Japan; and [b]Department of Ophthalmology and Vision Science and Department of Neurobiology, Physiology, and Behavior, University of California, Davis, Sacramento, CA 95817

Edited by Brian A. Wandell, Stanford University, Stanford, CA, and approved July 10, 2012 (received for review November 30, 2011)

The retinal image is sampled concurrently, and largely independently, by three physiologically and anatomically distinct pathways, each with separate ON and OFF subdivisions. The retinal circuitry giving rise to an ON pathway receiving input from the short-wave-sensitive (S) cones is well understood, but the S-cone OFF circuitry is more controversial. Here, we characterize the temporal properties of putative S-cone ON and OFF pathways in younger and older observers by measuring thresholds for stimuli that produce increases or decreases in S-cone stimulation, while the middle- and long-wave-sensitive cones are unmodulated. We characterize the data in terms of an impulse response function, the theoretical response to a flash of infinitely short duration, from which the response to any temporally varying stimulus may be predicted. Results show that the S-cone response to increments is faster than to decrements, but this difference is significantly greater for older individuals. The impulse response function amplitudes for increment and decrement responses are highly correlated across individuals, whereas the timing is not. This strongly suggests that the amplitude is controlled by neural circuitry that is common to S-cone ON and OFF responses (photoreceptors), whereas the timing is controlled by separate postreceptoral pathways. The slower response of the putative OFF pathway is ascribed to different retinal circuitry, possibly attributable to a sign-inverting amacrine cell not present in the ON pathway. It is significant that this pathway is affected selectively in the elderly by becoming slower, whereas the temporal properties of the S-cone ON response are stable across the life span of an individual.

koniocellular pathway | short-wave-sensitive cone pathways | visual psychophysics

One of the most basic properties of primate vision is that each point in the retinal image is sampled by at least three physiologically and anatomically distinct pathways (1, 2). These include a fast, high-contrast sensitivity, low-spatial resolution magnocellular pathway; and a slower, high-spatial resolution, chromatic parvocellular pathway. A third pathway, the koniocellular pathway, is color-opponent and slow, and it has poor spatial resolution. Overlaid onto the organization of these pathways are subdivisions into parallel ON and OFF systems (3). This originates at the first retinal synapse between the cone photoreceptor and the bipolar cell to give rise to the magnocellular or parvocellular pathways, resulting in further specialization and response selectivity for spatiotemporal luminance and/or chromatic increments (ON pathway) or decrements (OFF pathway). The assumption that detection of increments and decrements is mediated by separate ON and OFF pathways is supported by the work of Schiller et al. (4) in alert, behaving monkeys. During retinal infusion of the glutamate neurotransmitter analog 2-amino-4-phosphonobutyrate, which blocks synaptic transmission from cones to ON-bipolar cells but not OFF-bipolar cells, there is a profound loss in the ability to detect increments but not decrements. A number of other physiological (5) and psychophysical studies using adaptation (6) also support the view that increments and decrements are processed by different retinal pathways. Separate detection of short-wave-sensitive (S)-cone increments and decrements by different classes of cell is further implied by responses to temporally varying sinusoidal stimuli. Responses of S-cone ON and S-cone OFF cells in the lateral geniculate nucleus (LGN) of the marmoset are ~180° out of phase (7). In the psychophysical domain (8), selective adaptation of putative ON and OFF pathways can be shown following adaptation to sawtooth temporal modulation. If the polarity of the sawtooth adaptation is a rapid rise (or rapid fall), threshold increases are significantly higher for detection of increments (or decrements). If there were only one pathway for detection of increments and decrements, threshold changes would be the same regardless of the polarity of the sawtooth-adapting stimuli. A similar result was reported in our previous paper (9) using sawtooth adaptation of S-cone pathways, consistent with separate detection of S-cone increments and decrements by ON and OFF pathways, respectively.

Here, we characterize age-related changes in the responses to incremental and decremental stimulation of the S-cone pathways of the human visual system. The S cones synapse with a specialized S-cone ON bipolar cell (10) that provides the S^+ signal to a small bistratified ganglion cell that is opposed by middle-wave-sensitive (M) and long-wave-sensitive (L) cone signals (11). The search for a parallel S-cone OFF bipolar cell has been controversial (12–14), notwithstanding unequivocal evidence that a small population of ganglion and LGN cells codes an S-cone OFF response (7, 15). Recently, an S-cone OFF signal has been shown to provide input to a melanopsin-containing retinal ganglion cell (16). Although the retinal circuits originating from the S cones are controversial, it is known that their signals are carried by ganglion cell axons that project to distinct sublaminae (the koniocellular layers) in the LGN (17), which, in turn, project to cytochrome oxidase blobs in layers 2 and 3 of primary visual cortex (18, 19).

To characterize the temporal properties of putative S-cone ON and OFF pathways, we measured detection of stimuli along a tritan line, an axis of S-cone modulation, customized for each observer to increase or decrease S-cone excitation at equiluminance, such that the M and L cones receive constant stimulation (20). We found that the S-cone response to increments is faster than the response to decrements, but the latter response is even slower for older individuals. The slower response may be attributable to different retinal circuitry, possibly including mediation by an inhibitory amacrine cell synapse (21, 22) and/or a slow, melanopsin-containing retinal ganglion cell (16).

Results

To measure S-cone impulse response functions (IRFs), we determined each observer's isoluminance equation and tritan line (a line in color space that modulates only S cones). The latter was accomplished by color matching with a 420-nm adaptation field superimposed in Maxwellian view on the test patches from a computer monitor. The two-pulse thresholds were then measured for stimuli modulated in chromaticity along the tritan

Author contributions: K.S. and J.S.W. designed research, performed research, analyzed data, and wrote the paper.

The authors declare no conflict of interest.

This article is a PNAS Direct Submission.

Freely available online through the PNAS open access option.

[1]To whom correspondence should be addressed. E-mail: jswerner@ucdavis.edu.

This article contains supporting information online at www.pnas.org/lookup/suppl/doi:10.1073/pnas.1119770109/-/DCSupplemental.

line, at constant luminance, changing from the white background (Commission Internationale de l'Éclairage x,y = 0.33,0.33; 10 cd·m^{-2}) toward the short-wave spectrum locus to produce increments in S-cone excitation (detected by a putative ON pathway) or from the white point toward the long-wave spectrum locus to produce decrements in S-cone excitation (detected by a putative OFF pathway). The two pulses were 20.0–133.3 ms each and separated, the stimulus onset asynchrony (SOA), by 20–493.3 ms, yielding interstimulus intervals from 0–360 ms. Unlike previous approaches using an arbitrary blue stimulus (23, 24), this method modulates only the S cones.

Fig. 1 (*Left*) shows the S-cone increment and decrement thresholds for a younger observer and an older observer. We used the Burr and Morrone model (25) to compute the IRF. This model assumes the IRF follows an exponentially damped sine wave, and it was found to describe luminance IRFs with multiple bands well in our previous work (26). However, the S-cone IRFs are unimodal for both the putative ON and OFF systems, as seen in Fig. 1 (*Right*). The time to peak response is much longer than observed for luminance modulation and the duration of response is more protracted because of the lack of inhibitory response. This may be inferred as being attributable to postreceptoral pathways rather than to the S cones themselves, because their temporal properties are similar to those of M and L cones in primate retina (27).

The S-cone increment thresholds are lower than decrement thresholds, and consequently have higher relative IRF amplitude. The S-cone ON IRF always has higher amplitude and reaches peak amplitude before the S-cone OFF IRF. In Fig. 1, the putative S-cone ON response peak leads the S-cone OFF response peak by 37 ms and 96 ms for the younger and older observers, respectively. This is attributable to a slowing of the OFF response of the older observer. As can be seen from Figs. S1 and S2, this is typical of our entire sample of younger and older observers. These characteristics are also consistent with S-cone ON and OFF responses of single cells in the LGN and cortex of macaque monkeys (19). Fig. 2 summarizes the data from all observers. Despite individual differences in response magnitudes and time to reach the peak response, for every observer, the maximum amplitude is higher for the S-cone ON system, whereas the time to reach maximum response is shorter (as shown in Fig. S3). Student t tests and Wilcoxon signed-rank tests show that differences between the increment and decrement parameters are significant ($P < 0.01$), as are the differences between young and old observers in S-cone IRF amplitude and S-cone OFF rise time.

If the response under our conditions of measurement originates from the same photoreceptors for ON and OFF pathways, we might expect that the amplitude of the two IRFs would be correlated, and this is what can be seen in Fig. 3 (*Left*). This is consistent with similar responses from S cones to increments and decrements. We are not aware of direct measurements of isolated S-cone responses to increments and decrements; however, nonmammalian M and L cones undergo voltage excursions of approximately equal magnitude for intensity increments and decrements (28, 29), and this is likely to be the case for primate S cones, given their comparable temporal dynamics (27). Note that there are substantial individual differences in IRF amplitude; however, in each case, the ON and OFF amplitudes are correlated. The linear regression line shown for all observers is statistically significant (r = 0.93, $P < 0.001$). However, if the differences between ON and OFF IRF response times are attributable to different postreceptoral circuitry, we would not expect these parameters to be correlated. Fig. 3 (*Right*) shows that there is no systematic relation between these variables, and the slope of the linear regression line is not statistically different from zero. This fact not only supports the difference in postreceptoral circuitry between S-cone ON and OFF pathways but experimentally supports that our S-cone decrement pulse is exciting S-cone OFF pathways rather than the antagonistic L + M cone response in an S-cone ON pathway.

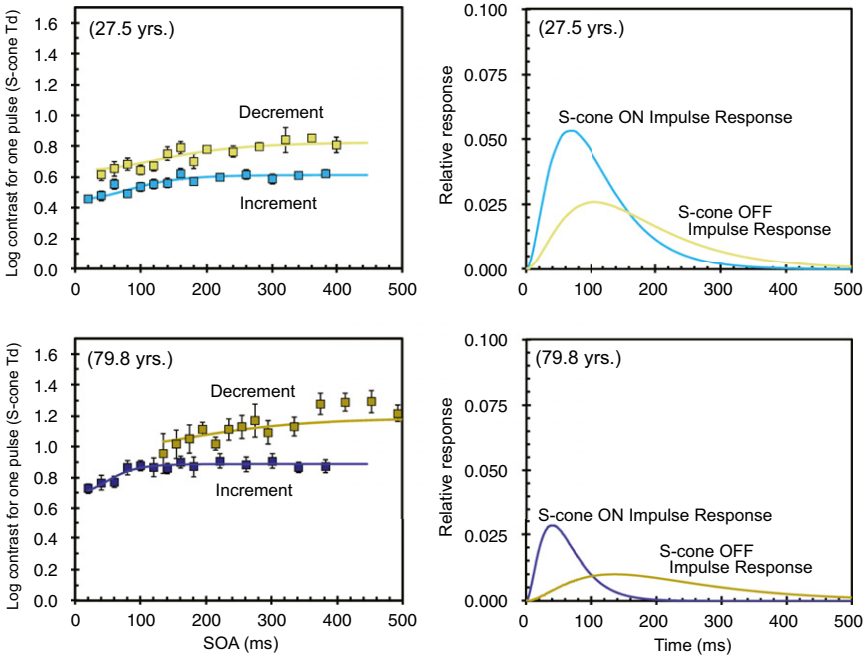

Fig. 1. Threshold data defined in terms of S-cone stimulation (S-cone Td) and the IRFs from one young observer (*Upper*) and one older observer (*Lower*). (*Left*) Log contrast thresholds for one pulse in S-cone Td as a function of the SOA. Blue squares and curves denote increment thresholds and model-fitting curves, respectively, obtained from the S-cone ON IRFs shown (*Right*). Yellow squares and curves denote decrement thresholds and the fit of the S-cone OFF IRFs. Error bars denote ±1 SEM. (*Right*) IRFs with the relative response plotted as a function of time. Bluish and yellowish curves denote S-cone ON (increment) and S-cone OFF (decrement) IRFs, respectively.

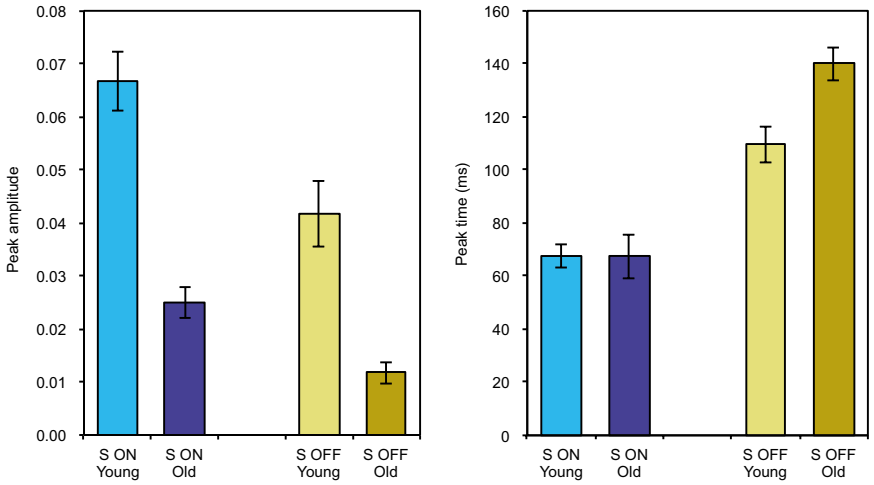

Fig. 2. Mean peak (maximum) amplitude (*Left*) and peak time (time at the maximum intensity) (*Right*) of young and old observer groups' S-cone ON and OFF IRFs calculated from the model. Error bars denote ±1 SEM.

Discussion

The small koniocellular fibers carrying S-cone signals to cortex should result in a slower time course for S-cone IRFs compared with luminance modulation (30, 31). Our studies confirm these temporal dynamics and provide a demonstration of selective age-related losses affecting a putative S-cone OFF pathway. Fig. 4 (*Left*) shows IRFs calculated from average data of each IRF from this study measuring S-cone increment and decrement responses compared with previously reported luminance-modulated IRFs, which are triphasic for most observers and likely mediated by a magnocellular pathway (26). For a linear system, these IRFs can be transformed to the temporal contrast sensitivity function (tCSF) by the inverse Fourier transform. These derived tCSFs are shown in Fig. 4 (*Right*). The tCSFs for chromatic modulation are low-pass, whereas the tCSFs for luminance modulation are bandpass. For S-cone ON and luminance tCSFs, the major difference between younger and older observers is in the amplitude. However, translation of the curves on the amplitude axis also results in shifts in the high temporal frequency cutoff. As a result, older observers will have lower cutoffs for both luminance and S-cone modulation. For the S-cone OFF system, the age-related change in the tCSF is not simply a scaling of amplitude. Older observers have a substantial loss in the temporal dynamics of their S-cone OFF pathway. As expected, however, sensitivities of S-cone ON and OFF are similar at lower temporal frequencies, keeping a balance in detection of changes between bluish and slower yellowish changes from white.

The S-cone system is thought to have evolved early and is a primordial pathway contributing to primate color vision (33). However, the S-cone OFF subdivision may contribute to additional functions other than color vision. OFF-type connections have been traced by electron microscopy from five S-cones to midget bipolar cells in macaques, which would, in principle, provide S-cone OFF input to a parvocellular pathway (13). However, in human peripheral retina (34), as in marmoset retina (14), synapses between S-cones and midget bipolar cells have not been found. In prescient speculation, Kolb et al. (34) suggested that perhaps the S-cone OFF signal is derived from an amacrine intermediary that receives its input from an S-cone ON bipolar cell. More recently, S-cone OFF responses from a giant sparse (wide-field) ganglion cell were found to be blocked by application of an ON pathway blocker (2-amino-4-phosphonobutyric acid) (12). This indicates that both types of response originate from the same S-cone bipolar cell. In the ground squirrel, a sign-inverting S-cone amacrine cell that receives input from S-cone bipolars and is able to provide glycinergic inhibitory input to downstream ganglion cells has been found (21, 22). These cells may thus provide the substrate to form the S-cone OFF ganglion cell.

Although our methods are psychophysical, and responses depend ultimately on the entire visual pathway, our interpretation

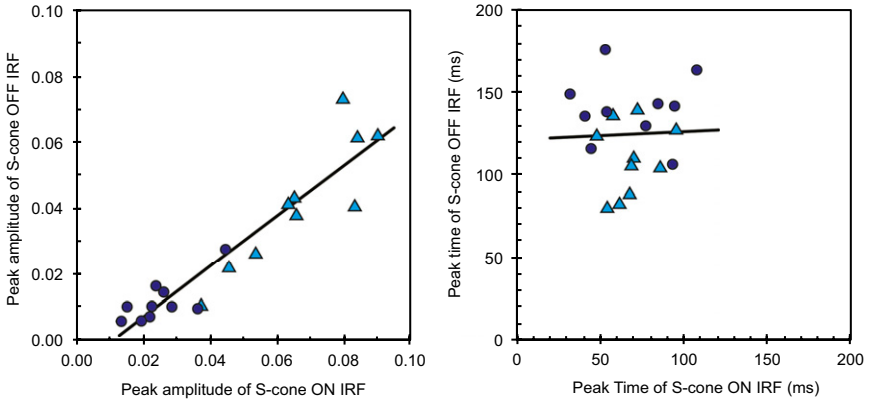

Fig. 3. Relations between S-cone ON and OFF IRFs for peak amplitude (*Left*) and peak time (*Right*). Triangles and circles denote the data points for younger and older observers, respectively. The lines are fitted by least-squares linear regression for all observers.

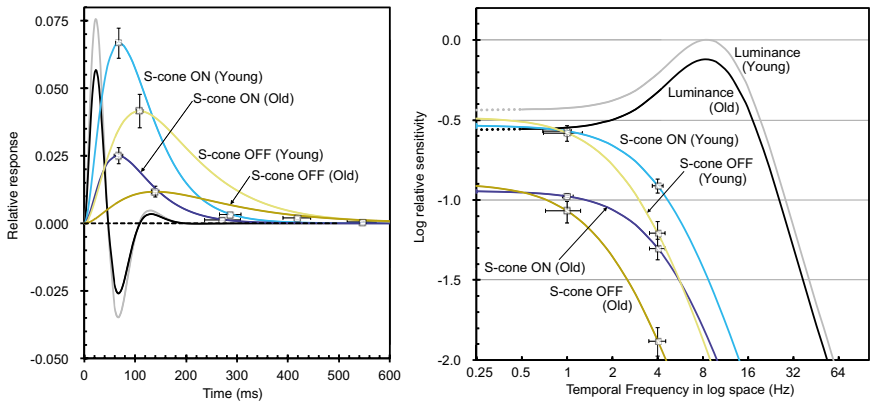

Fig. 4. (*Left*) Average IRFs for younger and older S-cone ON and OFF IRFs compared with luminance modulation from a previously published study using the same methods (26). The amplitude of luminance modulation is scaled down by a factor of 10 for purposes of illustration. Squares denote points at peak amplitude and peak time and at duration (5% intensity of peak amplitude). Error bars denote ±1 SEM. (*Right*) Corresponding tCSFs calculated from the inverse Fourier transform. Luminance and chromatic modulation were defined as the amplitude of the flicker sine wave divided by the mean luminance or chromaticity. Peak sensitivity of the luminance function is normalized to unity, and minimum sensitivity is defined as −2 log unit, corresponding to flicker modulation from 0.01 to 1 (32). Squares denote points at 1 Hz and 4 Hz for each function. Error bars denote the possible range of curves defined by ±1 SEM.

that the differences in response are mediated by retinal rather than upstream cortical circuits is supported by observations that retinal ganglion cells endow single units in the LGN of the primate with the fundamental properties that are observed in the psychophysical IRF here. Specifically, in the LGN, S-cone OFF cells are slower and have lower amplitude (impulses per second) than S-cone ON cells (7). A unique result of this study is that older observers differed from younger observers in the temporal dynamics of their S-cone OFF responses. It has been shown that there are age-related losses in cortical inhibitory connections of the primate (35) and feline (36) visual cortex. Specifically, losses in GABAergic inhibition are associated with senescent declines in cortical function, whereas its agonists improve single-cell stimulus selectivity in older animals. The present results suggest age-related losses also in the presumed inhibitory retinal circuit that contributes to human blue-yellow color vision.

Remarkably, at least some of the large ganglion cells carrying S-cone OFF signals are intrinsically photosensitive (16), and therefore may subserve additional functions, such as circadian photoentrainment. These intrinsically photosensitive retinal ganglion cells (ipRGCs) may be excited by S-cone modulation or through photon absorption by the melanopsin pigment found in the axons, proximal dendrites, and cell bodies of these neurons. Direct melanopsin-mediated activation of these cells from the stimuli used in the present study seems unlikely because the S-cone IRFs were much faster than the sluggish melanopsin-mediated responses and were obtained at lower light levels than found when rod and cone photoreceptor inputs are blocked (37, 38). If the age-related losses in the S-cone IRF are attributable to changes in the ipRGCs themselves, reduced responsivity to melanopsin stimulation may also be expected in natural environments. Anatomical evidence indicates that there is a loss in ipRGCs in the elderly (39). Further study is warranted to assess possible contributions of these ganglion cells to disorders of sleep and dysfunction of circadian rhythms, which become more common with increasing age (40) and have decreased stimulation by short-wave light as the result of age-related changes in the ocular media (41). In the present study, the reduced transmission of the ocular media in the elderly was controlled by equating stimuli at the level of the retina. As a result, the differences between young and old in the substrate for S-cone OFF response can be ascribed to neural factors. Losses in the neural substrate of S-cone OFF temporal responses in the elderly may be important under natural conditions not only for the retinal circuitry of color vision but for the evolutionarily more ancient function of regulating the biological clock (42).

Experimental Procedures

Participants. Ten young (6 male, 4 female, age range: 21.2–27.5 y) and 10 older (5 male, 5 female, age range: 65.5–82.4 y) observers completed testing. Before testing, each observer was screened to rule out the presence of retinal and optic nerve disease and abnormal ocular media. Visual acuity was ≥20/20 in the tested eye, and participants were refracted for the stimulus distance. Color vision was assessed as normal when tested with the Neitz anomaloscope, the Hardy–Rand–Rittler pseudoisochromatic plates, the Farnsworth F-2 plate, and the Cambridge Colour Test. Written informed consent was obtained following the Tenets of Helsinki and with approval of the Office of Human Research Protection of the University of California, Davis, School of Medicine.

Visual Stimuli. Visual stimuli were presented on a cathode ray tube (CRT) display (GDM-200 PS; Sony) operating at a 150-Hz frame rate that was controlled by a video board with 15-bit resolution (VSG 2/4; Cambridge Research Systems) using a Dell Pentium computer. A second CRT monitor displayed the stimuli for the experimenter.

The CRT was viewed through an astronomical telescope with a magnification of 2.16×. An aperture was placed before the telescope objective to form a 2.5-mm exit pupil in the plane of the eye pupil so that age-related changes in pupil diameter had no influence on retinal illuminance. Trial lenses were mounted in the spectacle plane to correct individual refractive error.

In adaptation conditions, a beam splitter combined the cathode ray tube (CRT) optical path with a Maxwellian-view optical channel to present a superimposed adapting field. The latter system used a 300-W xenon lamp and regulated dc supply. A neutral density wedge and neutral density filters were placed in a focal plane and collimated section of the beam, respectively. This system was calibrated at 420 nm, the central wavelength (8-nm bandwidth at half peak amplitude) of the interference filter placed in a collimated beam.

The observer was steadied with a dental impression bite bar that could be adjusted separately in *x-y-z* planes. An alignment channel was made possible by a pellicle placed in the optical path so that light from the subject's eye was directed into an auxiliary optical system. A reticule aligned with the optic axis of the telescope and Maxwellian view system permitted precise alignment of the eye pupil.

The CRT phosphors were calibrated spectrally using a spectroradiometer/photometer (model PR703-A; Photo Research) and radiometrically using a *p-i-n* 10 silicon photodiode and linear readout system (Optometer 81; United Detector Technology). Luminance was measured with a chromometer (CS-100; Minolta). The relation between phosphor radiance and voltage was linearized based on radiometric measurements and calibration software. Retinal illuminance was based on photometric calibrations following standard methods.

Each pulse had a Gaussian spatial profile, 2.26° diameter at 1 SD (106 pixels on a 640 × 480 pixel display), to eliminate artifacts caused by spatial transients. Rise and fall times of the CRT phosphors were measured with a photodiode and digital oscilloscope and were found to be ~1.2 ms for all phosphors. Given the diameter of the Gaussian patch, the decay of the test stimulus at the vertical scan frequency was <1.5 ms from the maximum. Peak-to-peak timing error of the SOA was <3%.

The stimuli were presented in one of four quadrants defined by a fixation cross, such that they were located 1.70° to one side or the other and 1.70° above or below the center of the fixation cross. S-cone increments and decrements were produced by modulating the two pulses equally in chromaticity at constant luminance toward short or long wavelengths, respectively, along the tritan line. The time between frames (interstimulus interval) was varied between 20 and 360 ms. Because of an insufficient dynamic range of the CRT phosphors, the pulses included additional frames for most observers to reach detection threshold. Control experiments using multiple frames demonstrate that this did not affect the results as long as the IRFs were calculated as the response to one-frame stimulation. This method of measurement and calculation assuming linear summation is justified because the double-pulse method itself has to use this assumption to obtain the IRFs. Fig. 1 and Figs. S1 and S2 display thresholds defined by one frame multiplied by the number of frames for one pulse.

Age-related increases in ocular media density affect the absolute and relative intensities of the broadband CRT phosphors at the retina in a complex manner (41). We estimated these effects after equating the phosphors by means of heterochromatic flicker photometry. An overall reduction in stimulus intensity attributable to age-related increases in ocular media has little effect on our results because we measured (logarithmic) contrast detection thresholds. For L-, M-, and S-cone stimulation, however, relative discrepancies between R, G, and B phosphors may introduce error in the calculated S-cone stimulation. The calculated relative discrepancy in terms of L-, M-, and S-cone log trolands are −0.011, 0.024, and 0.034, respectively, for a theoretical 80-y-old observer compared with a standard (32-y-old) observer. Thus, the accuracy of S-cone modulation in this study was sufficient even for the relatively broadband phosphors of the CRT.

Psychophysical Methods. ***Tritan lines.*** Individual tritan lines were determined by a metameric match in which S cones were suppressed by the presence of a superimposed 420-nm adapting field (3.52 log Td for the standard observer) presented in Maxwellian view. Four sets of two rectangular patches (1.2° × 0.6°, placed side by side) were superimposed on a 420-nm background (12°). The stimulus was an array of four test patches, with each corresponding to the approximate locations and size of the test stimuli used for two-pulse threshold measurements. The observer viewed a central fixation cross. The chromaticity of the two patches was complementary around the white point (equal energy), and the two patches were set as far apart in chromaticity space as possible within the gamut of the monitor.

Following 5 min of adaptation to the 420-nm field (12°), the observer was asked to find a match between the two patches by adjusting the intensity of one of the patches and varying the angle of the tritan line pivoted around the white point (thereby changing the chromaticity of both patches simultaneously). This match was determined five times, and the average angle defined the coordinates of the tritan line. Without S-cone adaptation, these patches did not match regardless of the angle of the line. Under the S-cone adaptation, however, all observers reported that they were able to find a metameric match between the squares.

Heterochromatic flicker photometry. Chromatic modulation of the IRF test probes was based on individual measures of isoluminance using 18-Hz heterochromatic flicker photometry with an annular stimulus (0.64°–2.77°, inner-outer diameter) corresponding to the test stimulus locations. The retinal illuminance ratio was measured for each of the three CRT phosphor combinations (R-G, G-B, and B-R).

Two-pulse thresholds. Two-pulse thresholds were measured after 5 min of dark adaptation and 5 min of adaptation to a 10-cd·m^{-2} equal-energy white background. Two pulses were presented on the screen, preceded by a high-pitched tone and followed by a low-pitched tone. The observer's task was to indicate in which of four quadrants the stimulus was detected by pressing one of four correspondingly arranged buttons. The stimulus was a chromaticity change in one Gaussian patch from equal-energy white along the individually determined tritan line. The four-alternative forced-choice (4AFC) task was combined with a two-down, one-up staircase in which staircases for each SOA were interleaved. Thresholds for each SOA were based on the last four of six reversals, corresponding to a 70.7% probability of detection. This was repeated in at least five to six sessions per observer.

Rod modulation. There are several reasons why rods would not be expected to contribute significantly to thresholds under our conditions of measurement. First, heterochromatic flicker photometry functions at the same retinal loci tested for S-cone increment and decrement thresholds revealed no departure from the photopic sensitivity function expected for young and older observers. Second, rods are much less sensitive than S cones to our stimulus modulation. Third, although rod input to small bistratified ganglion cells was demonstrated by Field et al. (43) at low scotopic luminances following 40 min of dark adaptation and recording from peripheral primate retina, they were unable to detect rod intrusion when their measurements were performed nearer the fovea and without a long period of scotopic adaptation. Thus, rod intrusion is not expected to influence our results because threshold detection is about 2° from the foveal center in the presence of a broadband background that is more than 50× the retinal illuminance used in most of the experiments conducted by Field et al. (43).

Data Analysis and Modeling. The double-pulse method is based on the assumption that the pulses sum to contribute to the threshold, provided the SOA is short enough to be integrated within the excitatory period of the detecting mechanism. If the SOA is longer than a critical duration, the response of the two pulses will not sum to contribute to the threshold, or the second pulse may produce a response that is combined during an inhibitory phase of the response to the first flash. Thus, the threshold for this double-pulse pair will increase. From the threshold change as a function of the SOA, the shape of the IRF can be estimated. We modeled the IRF as an exponentially damped, frequency-modulated sine wave as proposed by Burr and Morrone (25) using the following equation:

$$I(t) = a_0 H(t) t \sin\left\{2\pi\left[a_1 t(t+1)^{-a2}\right]\right\}\exp(-a_3 t) \quad [1]$$

where $I(t)$ is the impulse response as a function of time (t) and parameters a_{0-3} are positive, with a_0 defining the overall gain, a_1 the fundamental frequency of oscillation, a_2 the modulation frequency over time, and a_3 the steepness of the decay. $H(t)$ is the Heaviside function to ensure that $I(t)$ begins with a value of zero when $t < 0$ (1 when $t \geq 0$). Four parameters, a_{0-3}, were varied using a least-squares criterion, and in this way, the IRF could be fitted without any assumptions about the number of excitatory or inhibitory phases. This model has the advantage of fewer free parameters than other models of the IRF. It does not require the assumption that the impulse response is derived from a minimum-phase filter, although this assumption may be incorporated by setting $a_2 = 0$. Following the methods described in our previous papers on the IRF for luminance and S-cone modulation (20, 26), the fitted functions were based on a model of probability summation of visual response (44), $R(t,\tau)$:

$$R(t,\tau) = K[I(t) + H(t-\tau)I(t-\tau)], \quad [2]$$

where τ is the SOA, the interstimulus interval is $\tau-$ (pulse duration), and $H(t)$ is the Heaviside unit step function. K is the S-cone excitation level scaled as S-cone luminance of each pulse over the background S-cone luminance, and p, proportion correct, is:

$$p = 1 - (1-r)\exp\left(-\left[\int_o^T (R(t,\tau))^\beta dt\right]\right). \quad [3]$$

Parameter r is the probability attributable to chance (0.25 in this experiment), and parameter β, which determines the steepness of the psychometric function, was set to 4. T is the time to take the integral, which must be long enough for the response to be zero within the SOAs tested. We set T to 0.8813 s. The proportion correct at threshold, P_0, was $\sqrt{2}/2$, which is determined by the two-down, one-up procedure in the 4AFC method that we used. From Eqs. **2** and **3**, we obtained Eqs. **4** and **5** as:

$$K = \left[C \Big/ \left\{\left(\sum_{n=0}^{660}\left|I(n\Delta t) + H(n\Delta t\text{-}\tau)I(n\Delta t\text{-}\tau)\right|^\beta\right) * \Delta t\right\}\right]^{1/\beta}, \quad [4]$$

$$(\text{Log S-cone contrast at threshold}) = \log_{10}((10+K)/10), \quad [5]$$

where C is $-\ln[(p_0 - 1)/(r - 1)]$ (= $-\ln((4 - 2\sqrt{2})/3)$), Δt was set to 1.333 ms, and n was changed from 0 to 660 (0.8813 s). In Eq. **5**, S-cone luminance of the background becomes 10 S-cone cd·m^{-2} because we used a 10 cd·m^{-2} of equal-energy white as the background.

ACKNOWLEDGMENTS. This project was supported by the National Institute on Aging (Grant AG04058) and by the Japan Society for the Promotion of Science KAKENHI (Grants 20300081 and 24300085).

1. Lee BB (2011) Visual pathways and psychophysical channels in the primate. *J Physiol* 589:41–47.
2. Kaplan E (2004) The M, P, and K pathways of the primate visual system. *The Visual Neurosciences*, eds Chalupa LM, Werner JS (MIT Press, Cambridge, MA) pp 481–493.
3. Nelson R, Kolb H (2004) ON and OFF pathways in the vertebrate retina and visual system. *The Visual Neurosciences*, eds Chalupa LM, Werner JS (MIT Press, Cambridge, MA) pp 260–278.
4. Schiller PH, Sandell JH, Maunsell JHR (1986) Functions of the ON and OFF channels of the visual system. *Nature* 322:824–825.
5. Kremers J, Lee BB, Pokorny J, Smith VC (1993) Responses of macaque ganglion cells and human observers to compound periodic waveforms. *Vision Res* 33:1997–2011.
6. Chichilnisky EJ, Wandell BA (1996) Seeing gray through the ON and OFF pathways. *Vis Neurosci* 13:591–596.
7. Szmajda BA, Buzás P, Fitzgibbon T, Martin PR (2006) Geniculocortical relay of blue-off signals in the primate visual system. *Proc Natl Acad Sci USA* 103:19512–19517.
8. Krauskopf J (1980) Discrimination and detection of changes in luminance. *Vision Res* 20:671–677.
9. Shinomori K, Spillmann L, Werner JS (1999) S-cone signals to temporal OFF-channels: Asymmetrical connections to postreceptoral chromatic mechanisms. *Vision Res* 39: 39–49.
10. Mariani AP (1984) Bipolar cells in monkey retina selective for the cones likely to be blue-sensitive. *Nature* 308:184–186.
11. Dacey DM, Lee BB (1994) The 'blue-on' opponent pathway in primate retina originates from a distinct bistratified ganglion cell type. *Nature* 433:749–754.
12. Dacey DM, Peterson BB, Robinson FR (2002) Identification of an S-cone opponent OFF pathway in the macaque monkey retina: Morphology, physiology and possible circuitry. *Invest Ophthalmol Vis Sci* 43:2983 (ARVO e-abstr).
13. Klug K, Herr S, Ngo IT, Sterling P, Schein S (2003) Macaque retina contains an S-cone OFF midget pathway. *J Neurosci* 23:9981–9987.
14. Lee SCS, Telkes I, Grünert U (2005) S-cones do not contribute to the OFF-midget pathway in the retina of the marmoset, *Callithrix jacchus*. *Eur J Neurosci* 22:437–447.
15. Valberg A, Lee BB, Tigwell DA (1986) Neurones with strong inhibitory S-cone inputs in the macaque lateral geniculate nucleus. *Vision Res* 26:1061–1064.
16. Dacey DM, et al. (2005) Melanopsin-expressing ganglion cells in primate retina signal colour and irradiance and project to the LGN. *Nature* 433:749–754.
17. Hendry SHC, Reid RC (2000) The koniocellular pathway in primate vision. *Annu Rev Neurosci* 23:127–153.
18. Casagrande VA (1994) A third parallel visual pathway to primate area V1. *Trends Neurosci* 17:305–310.
19. Tailby C, Solomon SG, Lennie P (2008) Functional asymmetries in visual pathways carrying S-cone signals in macaque. *J Neurosci* 28:4078–4087.
20. Shinomori K, Werner JS (2008) The impulse response of S-cone pathways in detection of increments and decrements. *Vis Neurosci* 25:341–347.
21. Sher A, Devries SH (2012) A non-canonical pathway for mammalian blue-green color vision. *Nat Neurosci* 15:952–953.
22. Chen S, Li W (2012) A color-coding amacrine cell may provide a blue-Off signal in a mammalian retina. *Nat Neurosci* 15:954–956.
23. Uchikawa K, Yoshizawa T (1993) Temporal responses to chromatic and achromatic change inferred from temporal double-pulse integration. *J Opt Soc Am A* 10: 1697–1705.
24. Masuda O, Uchikawa K (2009) Temporal integration of the chromatic channels in peripheral vision. *Vision Res* 49:622–636.
25. Burr DC, Morrone MC (1993) Impulse-response functions for chromatic and achromatic stimuli. *J Opt Soc Am A* 10:1706–1713.
26. Shinomori K, Werner JS (2003) Senescence of the temporal impulse response to a luminous pulse. *Vision Res* 43:617–627.
27. Schnapf JL, Nunn BJ, Meister M, Baylor DA (1990) Visual transduction in cones of the monkey *Macaca fascicularis*. *J Physiol* 427:681–713.
28. Burkhardt DA (1994) Light adaptation and photopigment bleaching in cone photoreceptors in situ in the retina of the turtle. *J Neurosci* 14:1091–1105.
29. Normann RA, Perlman I (1979) The effects of background illumination on the photoresponses of red and green cones. *J Physiol* 286:491–507.
30. Field GD, et al. (2007) Spatial properties and functional organization of small bistratified ganglion cells in primate retina. *J Neurosci* 27:13261–13272.
31. Lee RJ, Mollon JD, Zaidi Q, Smithson HE (2009) Latency characteristics of the short-wavelength-sensitive cones and their associated pathways. *J Vis* 9(12):5.1–17.
32. Kelly DH (1961) Visual response to time-dependent stimuli. I. Amplitude sensitivity measurements. *J Opt Soc Am* 51:422–429.
33. Mollon JD (1989) "Tho' she kneel'd in that place where they grew..." The uses and origins of primate colour vision. *J Exp Biol* 146:21–38.
34. Kolb H, Goede P, Roberts S, McDermott R, Gouras P (1997) Uniqueness of the S-cone pedicle in the human retina and consequences for color processing. *J Comp Neurol* 386:443–460.
35. Leventhal AG, Wang Y, Pu M, Zhou Y, Ma Y (2003) GABA and its agonists improved visual cortical function in senescent monkeys. *Science* 300:812–815.
36. Hua T, Kao C, Sun Q, Li X, Zhou Y (2008) Decreased proportion of GABA neurons accompanies age-related degradation of neuronal function in cat striate cortex. *Brain Res Bull* 75(1):119–125.
37. Berson DM, Dunn FA, Takao M (2002) Phototransduction by retinal ganglion cells that set the circadian clock. *Science* 295:1070–1073.
38. Do MTH, Yau K-W (2010) Intrinsically photosensitive retinal ganglion cells. *Physiol Rev* 90:1547–1581.
39. La Morgia C, et al. (2010) Melanopsin retinal ganglion cells are resistant to neurodegeneration in mitochondrial optic neuropathies. *Brain* 133:2426–2438.
40. Cajochen C, Münch M, Knoblauch V, Blatter K, Wirz-Justice A (2006) Age-related changes in the circadian and homeostatic regulation of human sleep. *Chronobiol Int* 23:461–474.
41. Werner JS, Bieber ML, Schefrin BE (2000) Senescence of foveal and parafoveal cone sensitivities and their relations to macular pigment density. *J Opt Soc Am A Opt Image Sci Vis* 17:1918–1932.
42. Neitz J, Neitz M (2011) The genetics of normal and defective color vision. *Vision Res* 51:633–651.
43. Field GD, et al. (2009) High-sensitivity rod photoreceptor input to the blue-yellow color opponent pathway in macaque retina. *Nat Neurosci* 12:1159–1164.
44. Watson AB (1979) Probability summation over time. *Vision Res* 19:515–522.